Journal of Frailty, Sarcopenia and Falls

Original Article

# Submicrostructural domains in human secondary osteons

**Miroslav Petrtyl[1], Karel Balik[2], Ctibor Povysil[3], Margit Zaloudkova[2]**

*[1]Laboratory of Biomechanics and Biomaterial Engineering, Department of Mechanics, Faculty of Civil Engineering, Czech Technical University, Prague, Czech Republic; [2]Department of Composite and Carbon Materials, The Institute of Rock Structures and Mechanics, Academy of Sciences, Prague, Czech Republic; [3]Institute of Pathology, 1st Medicine Faculty of Charles University, Prague, Czech Republic*



**Abstract**

The cortical bone is a hierarchically organised biocomposite tissue ranging from the nanoscopic to the macroscopic scale. The present paper is concerned with the new morphological observations of human femoral cortical bone at the nanostructural/submicrostructural levels of older patients. The objective of this study is to verify and refine the descriptions of nanostructures and submicrostructures in selected localities of the human femoral diaphyses by the scanning electron microscope - Quanta 450 with the ETD detector. The great interest has been focused on identifying the orientations of basic structural domains of bones at each of their structural levels. The bearing structural domains are composed and oriented not only to effectively resist localized mechanical stresses/strains, but to *promote uniform dissipations of energy of deformation into lower structural levels of tissue*. As the domains of the 2nd structural level are mineralized nanofibrils, then dominant domains of the 3rd structural level are layered nanoshalls, creating the mineralized cylindrical columns, i.e. mineralized microfibres. Each mineralized nanoshell is composed of parallel oriented mineralized nanofibrils (nanorods). The nano/substructural elements are formed (during the bone remodeling) under the influence of the dominant biomechanical effects as are torsional micromoments, microforces in tension and/or in compression.

**Keywords:** Cortical bone, Histology, Secondary osteons, Nanoshall, Microfibers

## Introduction

The cortical bone is a highly dynamic connective tissue in which complex biomechano-chemical and bioelectrical (ionic) processes take place with the objective of maintaining the living bone tissue in a dynamic equilibrium. Dynamic loads predetermine the formation of new bone tissue and its long-term function stability. The structure of bone tissue at all its structural levels reflects its response to dominant stress/strain states. Bone tissue structures are adapted to dominant loading effects during bone tissue remodeling processes. Therefore, great interest has been focused on identifying the orientations of basic structural units (structural domains) of bones at each of their structural levels[1].

The biomechanical loading of bone tissue primarily affects its modeling and remodeling at all its structural levels[2]. Through metabolic processes, the loading effects primarily regulate the optimal strength of tissue, its elasticity, viscosity and the formation of complex heterogeneous, composite structures. At each structural level of the diaphyseal cortical bone, the bearing elements are composed and oriented not only to effectively resist localized mechanical stresses, but also to *promote uniform dissipations of energy of deformation into lower structural levels of tissue*. Each i-th structural level is composed of a complex (system) of structural units of a lower (i.e. i - 1) structural level being simultaneously a basic structural unit of a higher (i.e. i + 1) structural level (Table 1).

At each level of the hierarchy of cortical bone structures, the basic structural units have a genetically predetermined position and primary orientation. During remodeling cycles, the orientation of numerous structural units undergoes changes. From a biomechanical perspective, they depend on the magnitudes and directions of dominant principal stresses, or the directions of dominant principal deformations. With

*The authors have no conflict of interest.*

***Corresponding author:*** *M. Petrtyl, Laboratory of Biomechanics and Biomaterial Engineering, Department of Mechanics, Faculty of Civil Engineering, Czech Technical University, Thakurova 7, 160 00 Prague 6, Czech Republic*

***E-mail:*** *petrtylmir@seznam.cz.*

***Edited by:*** *George Lyritis*

***Accepted*** *31 August 2016*

| NANOSTRUCTURE | | | SUBMICROSTRUCTURE | | MICRO-STRUCTURE | MEZO-STRUCTURE | MACRO-STRUCTURE |
|---|---|---|---|---|---|---|---|
| 1. level | 2. level | 3. level | 4. level | 5. level | 6. level | 7. level | 8. level |
| < 1μm | | | 1 – 10 μm | | 10 – 500 μm | 500 μm – 10 mm | ➢ 10 mm |
| tropocollagen molecule + HA crystal /crystals | system of sub-nanofibrils | system of parallel mineralized nanofibrils | system of mineralized nanoshalls | system of mineralized microfibres | system of osteonal lamellas | system of osteons | femoral bone |
| 50x25x3 nm 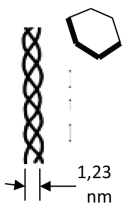  | 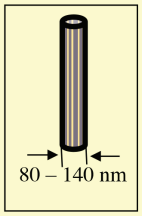  | 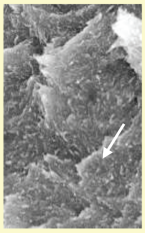 |  |  |  | 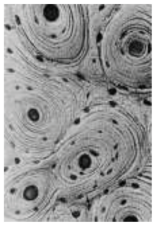 | 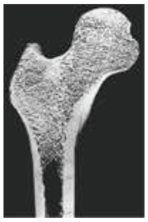 |
| subnanofibril (diameter of 1,23 nm) | mineralized nanofibril (nanorod), diameter of ca 80 - 140 nm | mineralized nanoshall | mineralized microfibre (micro-column) | lamella of osteon (mineralized column wall) | osteon | population of osteons | proximal diaphysis |
| structural domains | | | | | | | |

**Table 1.** Structural levels in cortical bone.

respect to some more or less varying descriptions of the structures of secondary osteons, considerable attention has been paid to histological descriptions of microstructures and nanostructures.

Initial pioneering research studies focusing on the orientation of collagen fibres in the lamellae of secondary osteons were conducted by Ebner (1874), Gebhardt (1901, 1906)[3] and Weidenreich (1930)[4]. In mutual agreement, they confirmed the harmonic alternation of lamellae with longitudinal microfibres (parallel to the longitudinal axis of the osteon) and lamellae with transverse microfibres (lying in planes roughly perpendicular to the longitudinal axis of the respective osteon). In 1887, Ranvier[5] described the structures as "homogeneous" lamellae alternating (without specifying the orientation of fibres) with lamellae containing short fibres lying in them in coaxial cylindrical layers. A similar conclusion was also reached by Ziegler (1908), who replaced the term "homogenized" lamella with the term "interstitial substance"[6].

Ruth (1947) confirmed the harmonic alternation of osteon lamellae[7]. He claimed that a loose (diffusion) lamella with randomly oriented fibres was situated between any two "compact" lamellae. He considered the loose lamella wider than the observed adjacent "compact" (fibrous) lamellae. Ruth described the cross-linking of randomly oriented collagen fibres in looser lamellae with adjacent "compact" lamellae containing unidirectionally oriented mineralized microfibres.

In 1952 and 1956, Rouillier et al.[8,9] published a model similar to the Ruth's model. He stated that fibres from adjacent (loose) lamellae, randomly entered into compact lamellae.

A different view of the lamellar structure was introduced in 1961 to 1973 by Ascenzi and Bonucci[10-14]. They claimed that each successive - adjacent lamella contained mineralized collagen fibres oriented in the direction of the helix in the way that right-handed oriented collagen fibres in one lamella alternated with left-handed collagen fibres in the successive adjacent lamella. The principal lamellar structures in juvenile and adult human bone were described in 1986 by Reid[20]. In 1988, Marotti and Muglia characterised the lamellar structures of osteons[15] by pointing out the harmonic alternation of two types of lamellae, i.e. "thin" ("dense", dark) lamellae rich in "intertwined" fibres and "thick" lamellae (with distinctly looser intertwining of mineralized type I collagen fibres), observable in them.

In 1993-2013, Marotti et al.[16-19,21] used the polarized light microscope (PLM), the scanning electron microscope (SEM) and the transmission electron microscope (TEM) to compare the previous findings of his colleagues related to the orientations and structures of bones. They confirmed the proximity of theirs group's findings to the conclusions published by Gebhardt[3]. In 1999 (and 2003), the previous

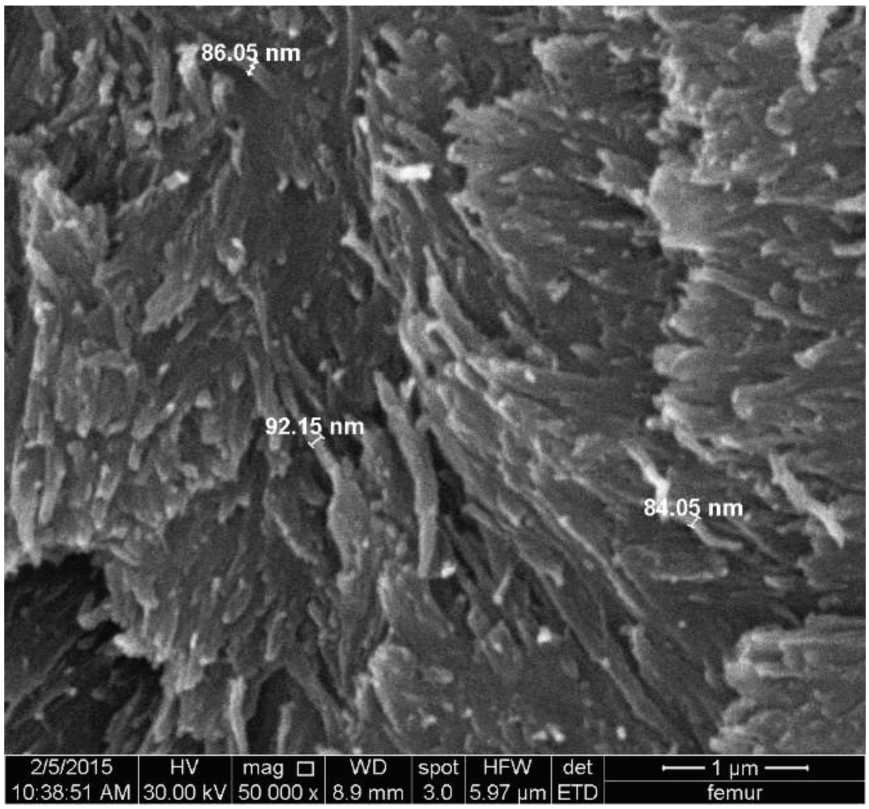


**Figure 1.** Systems of mineralized composite nanofibrils (nanorods) ca 80 to 140 nm in diameter, magnification of 50 000 x. Each nanofibril is a constitutive domain of the 2nd structural level.

findings of Ascenzi's (A.) group were further refined by Ascenzi (M.G.) et al.[14,51], who described Circularly Fibred Osteonic Lamellae. In 2013, Marotti et al.[17] characterised the problem of bone lamellation as the attempt to explain different proposed models.

In 1988, Giruad-Guille et al.[22,23] introduced the TPA (Twisted Plywood Architecture) model consisting in the rotation of parallel collagen fibres around the osteon longitudinal axis in sublayers (i.e. sublayers within each lamella). The follow-up to Giruad-Guille's work[22,23] are studies by Hofmann et al.[24] from 2006, and Wagermaier et al. from the same year[25], who confirmed the non-linear structures of microfibres in bone lamellae.

Given that different findings appear in the descriptions of the microstructures and submicrostructures of the human cortical bone, we have focused on refining the bone tissue structures particularly at the 2nd to 5th structural levels, (Table 1, *the yellow area*).

In this context, it should be noted that new structures of secondary osteons in the cortical bone, their properties and behaviour in the biomechanical and histological perspective (at individual structural levels) are also affected by previous remodeling cycles. Each newly arising tissue structure (in a specific macroelement) is nearly always affected by the biomechanical properties of surrounding tissues which were not resorbed, but are the remains of tissues from older remodeling cycles. The bearing structures of the cortical bone and their orientations allow deriving the ways of transferring dominant loads to lower structural levels at individual hierarchical levels, finding the directions of dominant loads and thus confirming or reconsidering some previous conclusions on the observed structures.

The objective of this study is to verify and refine the descriptions of nanostructures and submicrostructures of the older human diaphyseal compact bone (in selected localities of the human femoral diaphysis) with the scanning electron microscope and, based on the observed structures, successively biomechanically assess what principal types of combined loads can be transferred by individual nanostructural and microstructural domains.

## Materials and methods

Bone tissue structures are mostly studied using optical microscopes, polarizing light microscopes, scanning

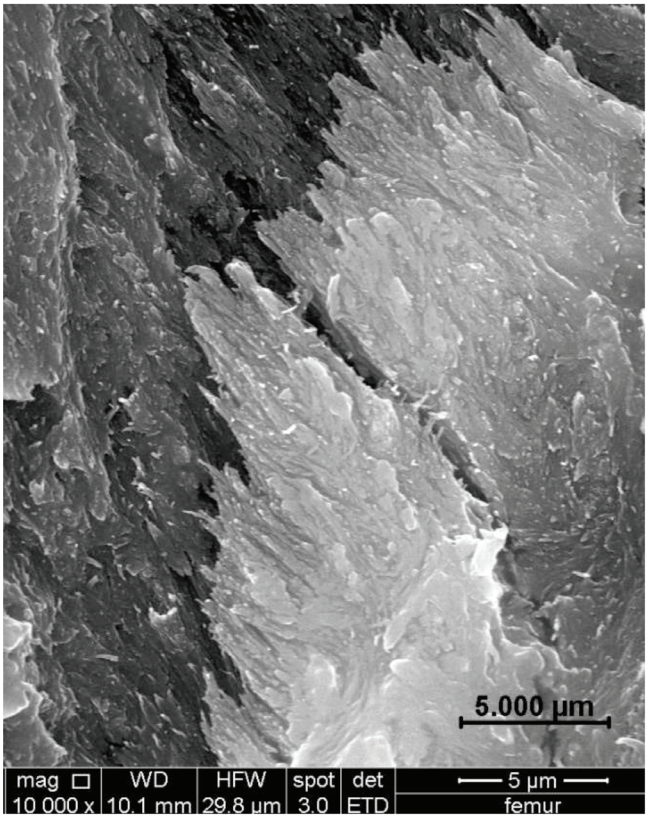


**Figure 2.** Bundles of mineralized nanofibrils (nanorods) 80-140 nm in diameter from the cleavage of an osteon part. In the top right part of the image, the parallelism of the longitudinal axis of nanofibrils and their lamination are clearly visible, magnification of 10 000 x. System of nanofibrils (with the same orientation) create the mineralized nanoshall that is the constitutive domain of the 3rd structural level.

electron microscopes, imaging methods based on magnetic resonance imaging, computed tomography, etc. Each imaging device provides specific conditions for observations which another device lacks, or only meets to a limited extent. Consequently, it happened that some structures were described with less accuracy or incompletely, which was not the researcher's fault.

In a broader context, it cannot be overlooked that highly specific, less common and sometimes even unique heterogeneous composite structures may be observed in bone tissues after several remodeling cycles. This is affected by the transformations of heterogeneous media which arose in previous remodeling cycles. Besides, the osteogenic activities of a new generation of osteoblasts reacting in each new remodeling cycle to the residua of the unresorbed surrounding medium are manifested. Thus, for example, it happens that the populations of new osteons (at the 7th structural level) are very different in shape from the generation of nearby, but older osteons generated in the previous remodeling cycle.

Guided by the objectives of our studies, we used the QUANTA 450 scanning electron microscope with the ETD (Everhart – Thornley) detector. The observation of structures was focused on fracture interfaces in osteons in 18 cortical bone specimens removed from the lateral walls of human femoral diaphyses, about 5 mm from the periost and at the level of the plane perpendicular to the longitudinal femoral axis lying ca 13 cm distally from the vertex of the femoral head of each right femur. The analyses were made on femurs of men *aged 56, 64 and 66 years*. The selection of cleavage localities and the scanning of suitable bone tissue specimens in the preparatory phase (before observations) were performed with the classic optical microscope. The main observations were performed under the Quanta 450 scanning electron microscope using accelerating voltage of 30 kV, at a working distance of 6-10 mm depending on the required magnification ratio. Several dozen localities at the 2nd to 6th structural levels (Table 1) were systematically observed and analysed. The secondary electron imaging mode on the Everhart-Thornley detector was used during the observations. Images at magnification ranges of 1.000x to 50.000x were used for the descriptions of structures.

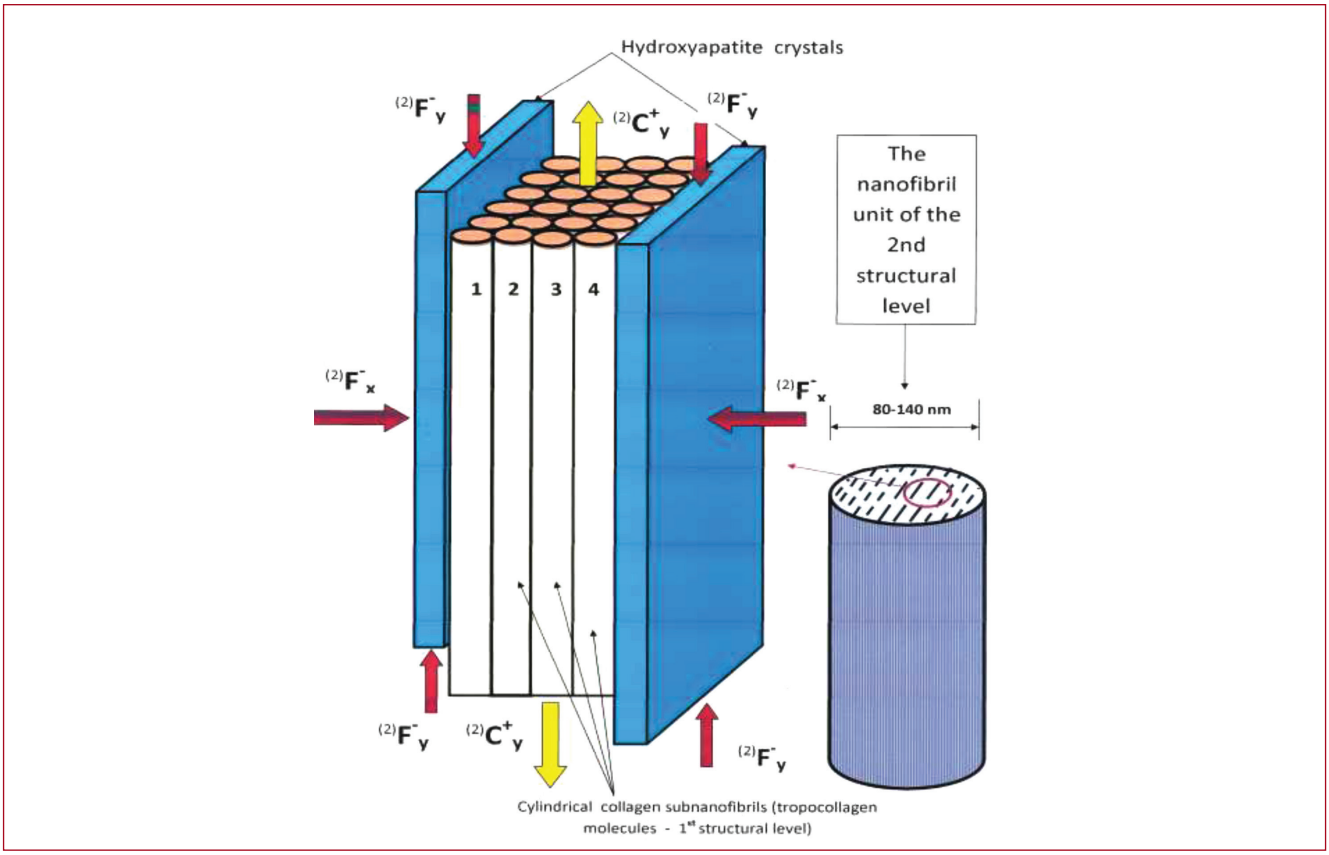


**Figure 3.** A schematic diagram illustrating the assembly of collagen subnanofibrils with bone HA crystals (left part of the image) and the nanofibril domain of the 2nd structural level (right part of the image).

Specimens fixed in carbon paste and gold-plated in an argon atmosphere were prepared to study the osteon structures of the cortical bone using scanning electron microscopy. The above treatment produced a thin conductive layer of gold on their surface and imaging in the high vacuum regime, in the order of $10^{-4}$Pa, could be used where the scanning electron microscope reaches the highest resolution.

The method of the observation and study of structures at cleavage interfaces allowed observing the cleavage surfaces of structural elements, the shapes of separated parts of tissues starting from the 2nd level of the cortical bone nanostructure very well (Table 1).

## Results

### *NANOSTRUCTURES – 1st, 2nd and 3rd structural level*

The basic constitutive domains at the 1st structural level (Table 1) are elementary supramolecular units – subnanofibrils, 1.23 nm in diameter and 300 nm in length. Each subnanofibril is connected in series with another subnanofibril (of the same length) by means of HA crystals in the direction of longitudinal axis of subnanofibrils[26,27]. These elementary linear aggregates (collagen I type tropocollagen molecules interconnected in "chains") form a higher structural unit with hydroxyapatite crystals at the 2nd structural level[30,32,33,39] and a mineralized nanofibril (mineralized *nanorod*). The diameters of each fibril (according our measurements) range in the interval of ca 80 to 140 nm, (Figure 1).

It is evident from Figure 1 that adjacent and nearby parallel mineralized nanofibrils tend to form a laminated system of nanorods. The parallelism of the longitudinal axes of mineralized nanofibrils is very clearly visible at cleavage interfaces, Figure 2. The rough schematic of the complex model of subnanofibrils and HA crystals at the 1st and the 2nd structural level is evident from schematic Figure 3[26,31,34]. Tropocollagen molecules are interconnected with HA crystals in the longitudinal direction and with HA polycrystalline plates in the transverse direction[26,31,34]. The straight or arcuate axes of nanofibrils in the same nanolayer are usually parallel. Some parallel nanofibrils in adjacent nanolayers, however, may have a *different orientation*. Nanofibrils are grouped into laminated arcuate or planar *nano/microshells* (Table 1 and Figure 4).

The groups of parallel nanofibrils (*nanorods*) form a


**Figure 4.** Systems of vertically arranged mineralized microfibres. Each one is a constitutive domain of the 4th structural level. Mineralized microfibres are created by nanoshalls.

fundamental structural domain (unit) of the 3rd level, i.e. a *mineralized shell*. Mineralized shells (according to our observations) form *multi-laminated structures* (Figure 5). The nanofibrils in these oval/circular shells are helically oriented mostly. Their steepness increases in osteon lamellae, which are situated closer to the Haversian canal. The cleavage interfaces of osteon nanostructures/submicrostructures allow observing not only the orientations and fracture faults of individual nanofibrils (at the 2nd structural level), but also the surface cleavage of mineralized nanoshells (at the 3rd and 4th structural level).

Figure 4 clearly shows parallel rotating laminated *coaxial shells, which gradually "wrap" each other*. They form *mineralized columns* – mineralized microfibres. The microfibres have a roughly circular/oval cross section. The crosslinking of the microfibres (columns) by means of laminated mineralized fans is evident in Figure 5 and Figure 6. The surface separation of laminated mineralized nanoshells allows drawing a hypothesis that the cortical bone osteogenesis produces the gradual lamination of nanoshall at nanostructural levels.

## *SUBMICROSTRUCTURE – 4th structural level*

The basic structural domain at the 4th structural level of the cortical bone are mineralized microfibres (*microcolumns*), Figure 4, Figure 6 and Figure 7. Their diameters range around ca 5-8 µm. They may reach lengths of up to several dozen µm. Mineralized microfibres are shaped like cylindrical columns composed of annular shell segments. In the lamellae near the osteon's central axis, the oval cross sections of microfibres (*microcolumns*) become more flatter, more segmented, and mineralized shells form laminated planar or only slightly arched systems.

The mineralized microfiber (*microcolumn*) is composed of multi-laminated mineralized shells mutually overlapping each other (Figure 5). The longitudinal axes of the microfibres (*microcolumns*) in the same lamella (*microcolumn wall*) are mostly parallel, while in the adjacent lamella their inclination mostly differs. Each microfibre is bonded to the adjacent microfibre by means of nanoshells. The cross-linking of individual microfibres is provided for example by fan-shaped mineralized shells (Figure 5, Figure 6).

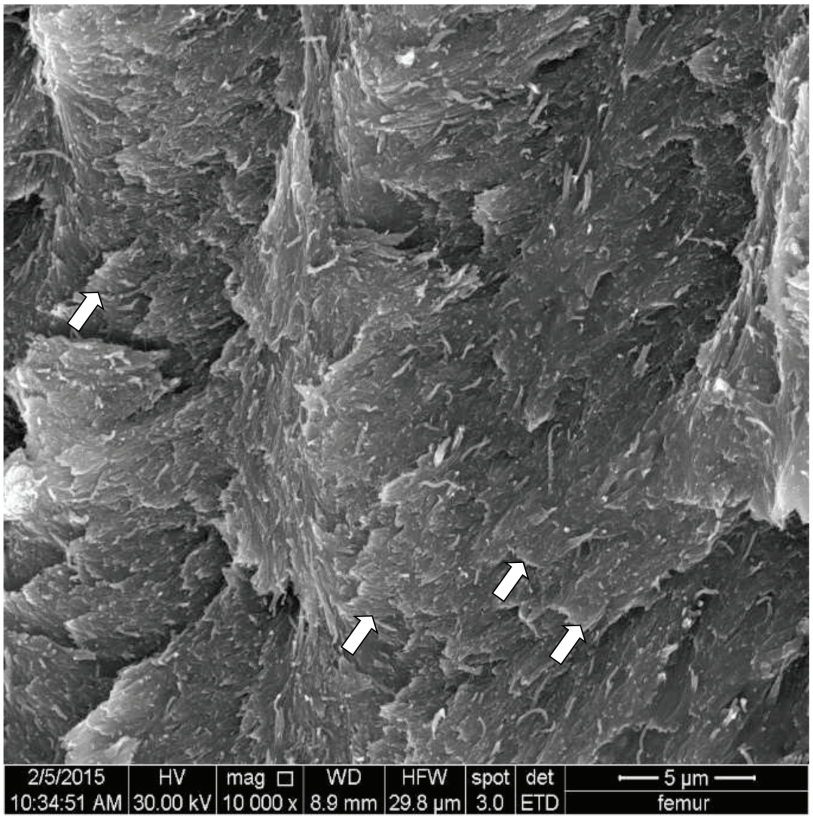


**Figure 5.** Magnified mineralized nanoshells (arrows) form mineralized columns – microfibres. Each nanoshell is the fundamental constitutive domain of the 3rd structural level, magnification of 10 000 x.

### *SUBMICROSTRUCTURE – 5th structural level*

The systems of mineralized microfibres form a lamella (*a column osteon wall*) at the 5th structural level (Figure 7, Figure 8). The longitudinal axes of the microfibres lying in the same lamella are roughly parallel in orientation. In the adjacent concentric lamella (of the same osteon), the longitudinal axes of microfibres, in the direction towards the longitudinal axis of osteon, usually have a steeper inclination, which further increases in each successive lamella in this direction.

In Figure 8, the separated part of osteon specimen clearly shows lamellae composed of *microcolumn walls*. The lamellae are formed by mineralized *microcolumns*, resembling filled up ocarina or organ pipes by their shape. The space between two adjacent lamellae (column walls) termed a "stronger/wider lamella", "loose lamella" in literature[7,15-18] is not a lamella in fact. It is a space which is very loosely filled up with stabilizing laminated bridge/cantilever shells or arcuate bindings which span the interlamellar space and provide transverse (radial) stability of mineralized microfibres (or column walls). The column structure of lamellae is evident from Figure 6 and Figure 8. The vertical radial mineralized shell partitions/bindings which stabilize adjacent lamellae are clearly visible.

The lamellae of secondary osteons at the 5th level are structured so that they may transfer combined loads, i.e. combined effects of external torsion moments, external bending moments and tensile/compressive normal forces. The higher structural complexity in the structural domains contributes to the higher quality of transfer and dissipation ability of loading effects into lower structural levels.

## Discussion

The cortical bone is a hierarchically organised biocomposite tissue ranging from the nanoscopic to the macroscopic scale. The living bone tissue, like other biological systems, has the ability of optimizing these structures at all "its" structural levels, optimizing their functions and their behaviour. The cortical bone is a multi-functional biological tissue possessing, in the biomechanical perspective, a bearing and, in numerous cases, also a protective function (fully or partially covering soft connective tissues and organs). The excellent biomechanical characteristics of bone tissue at all its structural levels are the result of tissue adaptation to its external loads.

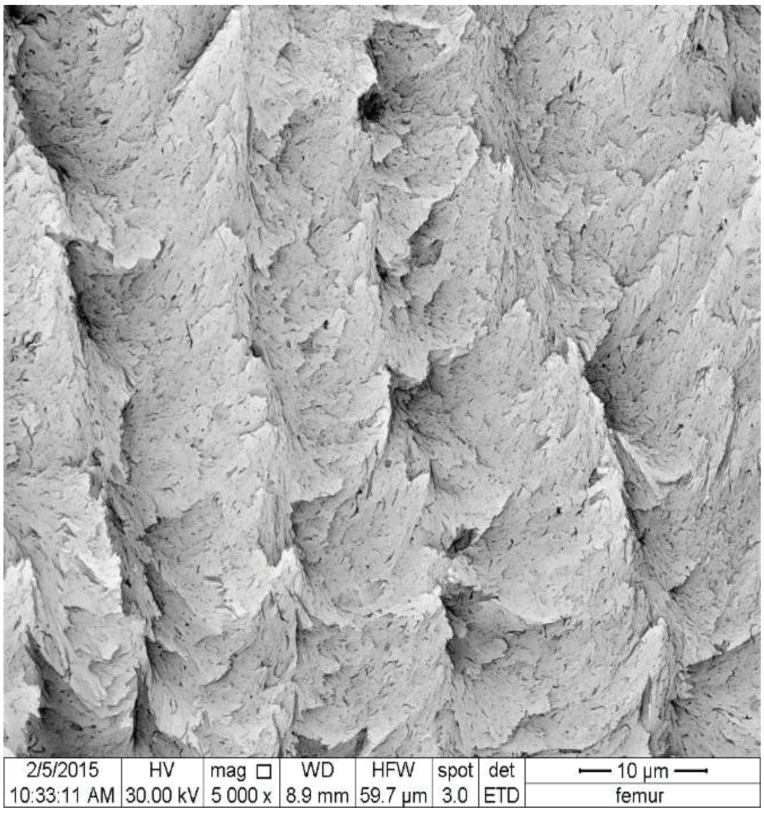


**Figure 6.** (negative) Systems of laminated and vertically arranged mineralized nanoshells creating the microfibre. Each nanoshell (as a domain of the 3rd structural level) is a constitutive element of the 4th structural level, i.e. of a mineralized microfibre (microcolumn), magnification of 5000 x. The fan-shaped cross-linking of mineralized microfibres is evident between the mikrocolumns.

Bone tissue allows dissipating and transforming potential energy of deformation from the highest structural level to the lowest structural level very efficiently. Whereas at the highest structural level, for example, the femoral diaphysis is loaded by variations of combined loads during moving (i.e. combinations of normal and shear forces, bending moments and torsion moments), at the lowest structural levels, due to the adaptation of structures to dominant loading effects, simple loading occurs, i.e. the nanostructure elements are loaded in the simplest possible way: in simple tension and/or simple compression. In other words, the hierarchical structures of the cortical bone allow dissipating potential energy of deformation to lower structural levels gradually and very efficiently so that the structures at the lowest structural levels are locally loaded least of all and in the simplest way, i.e. in simple tension and/or simple compression.

The fundamental structural units of bone tissue at the nanolevel are tropocollagen subnanofibrils, hydroxyapatite (HA) crystals, water, non-collagen bone proteins (NBP) and specific free ions. The tropocollagen subnanofibrils are 1.23 nm in diameter and 300 nm in length[35,39,40]. The positions of HA crystals at all structural levels, or the orientations of three polar principal axes of symmetry and one non-polar principal axis of symmetry play two key (and irreplaceable) roles, i.e. the biomechanical and bioelectrical role. Due to the fact that HA crystals possess high strength in compression of up to 206-896 MPa and in tension of ca 69-193 MPa[55], at nanostructural levels these crystals are so oriented to reliably transfer local dominant (nano) compressions/(nano) tensions. Tropocollagen subnanofibrils at this level have the opposite mechanical function, i.e. transferring local dominant tensile (nano)forces.

By loading HA crystals in compression, the piezoelectric effect occurs in bone tissue, i.e. (+/-) ions are generated. Water is an important bone component at all structural levels. Free ions contained in water regulate metabolic processes through cells and, successively, the production of type I collagen tropocollagen molecules. In terms of biomechanics, water also contributes to the *hydraulic strengthening of bone tissue*.

The two above mentioned highly specific roles of HA crystals, i.e. the transfer of dominant compressive loads (or accumulation of potential energy of deformation) and production of (+/-) ions, predetermine the places and positions of HA polycrystalline blocks, columns and

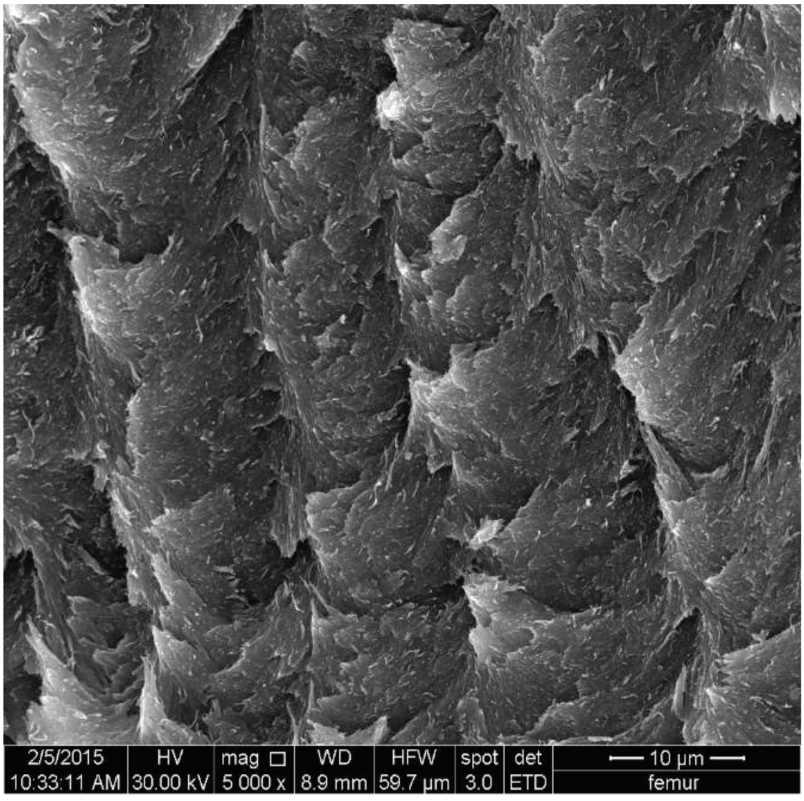


**Figure 7.** Mineralized and parallel concentric segmented nano/microshells form the microfibres having the column-shaped approximately. The mineralized microfibres create the column wall, i.e. the osteon lamella, magnification of 5 000 x.

nanoplates at nanostructural levels. HA crystals are placed between the ends of tropocollagen subnanofibrils and, according to[44], in irregular columns on the circumference of the tropocollagen helix[39,41,50].

The helical structure of tropocollagen subnanofibrils and the bonding forces between molecules predetermine the fundamental behaviour of nanofibrils at higher structural levels. Type I collagen has the ability of excellent transformation due to the effect of tensile loading in the longitudinal direction of subnanofibrils and accumulation of energy of deformation. This property is utilized in loaded type I collagen subnanofibrils at all structural levels. Thus, in terms of biomechanics, discrete elastic helical collagen subnanofibrils (without any other structural components) are able to transfer *tensile loads*. The (discrete) tropocollagen subnanofibril alone, without bonds to other structural components (HA), however, is unstable in compression in the direction of its longitudinal principal axis of symmetry. This drawback was compensated by nature in a sophisticated way. At the 1st structural level, the ends of tropocollagen molecules were connected with HA crystals, which, together with longitudinal polycrystalline HA columns and polycrystalline HA nanoplates (see the 2nd structural level below), can transmit local *compressive loads*. Despite the numerous studies available focusing on the mineralization of collagen, the molecular mechanism of mineralization at the 1st structural level has not been quite reliably elucidated yet[45]. As type I tropocollagen molecules themselves cannot induce crystallization, it is considered that the key role is played by non-collagen proteins (osteonectin and osteocalcin), which contribute to the stabilization of the amorphous phase of the nanoprecursor, which is calcium-phosphate[28,29,35].

The presence of HA crystals (between the heads of tropocollagen molecules and along their longer sides[25-27,35]) substantially increases the total rigidity of the composite at the 1st hierarchical level and, successively, contributes to reaching the stability of structures at the 2nd structural level.

Subnanofibrils 300 nm in length are interconnected via HA crystals along their longitudinal dimension. The crystals fill up the space between the heads of adjacent subnanofibrils 40 nm in length[26,44] and [27] (Figure 3). In this way, chained subnanofibrils can exceed ca 1 µm in length arise. Another (adjacent) "long" subnanofibrils and, successively, another "long" subnanofibril, etc. create the plane system of subnanofibrils[30,31]. The subnanofibrils create the ("first") layer (nanowall) of chained subnanofibrils. The adjacent

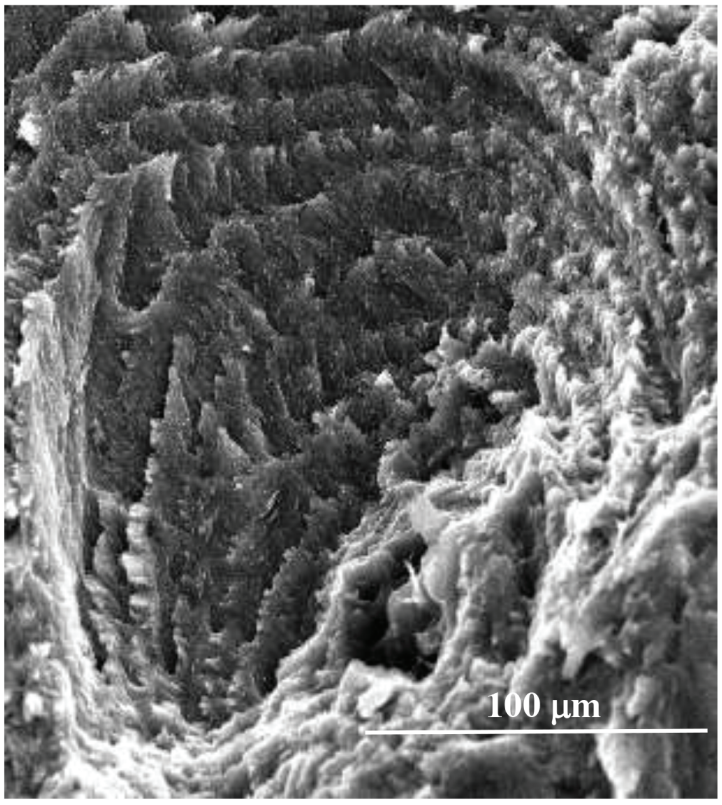


**Figure 8.** Cleavage of an osteon part with a distinct lamellar structure of vertical mineralized microfibres, scale of 100 µm.

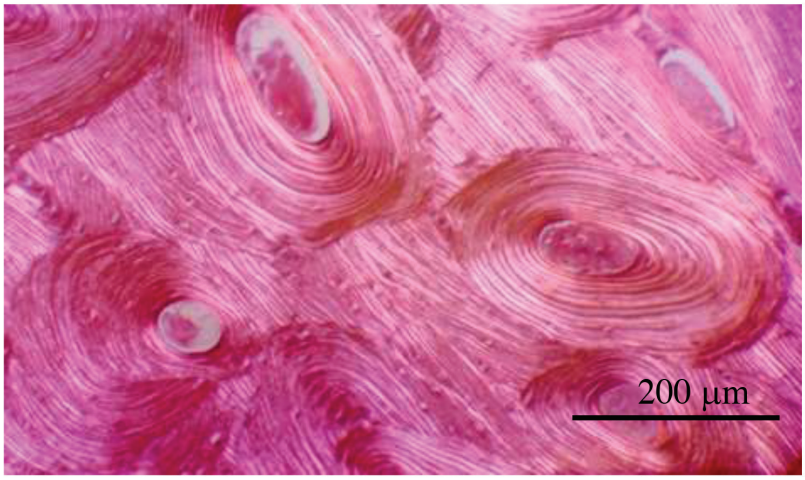


**Figure 9.** Photomicrograph of a cross section of a normal cortical bone with numerous Haversian systems. There are demonstrated concentric lamellae by their birefringence in the polarized light. Each osteon is the constitutive domain of the 6$^{th}$ structural level of bone, scale of 200 µm.

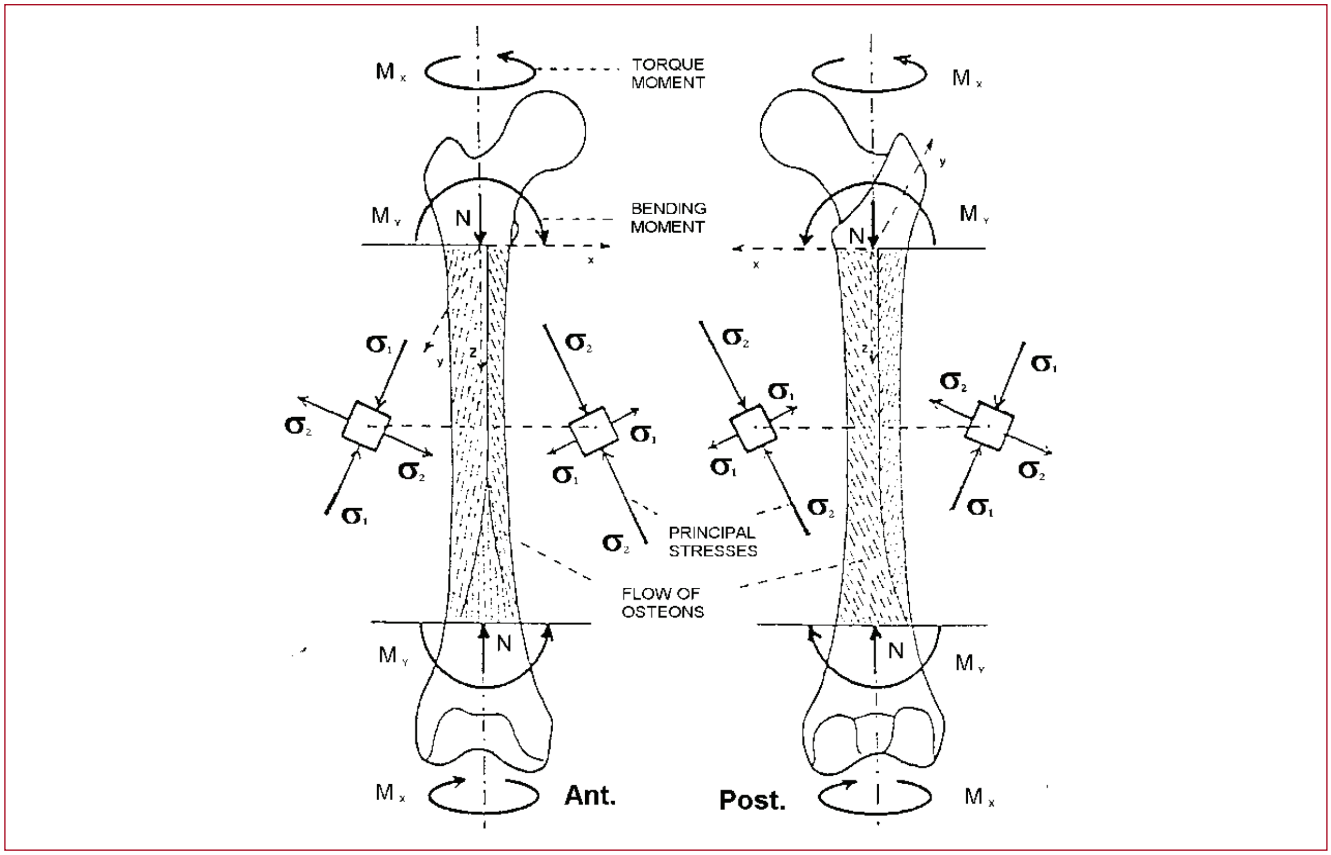


**Figure 10.** Longitudinal axes of osteons in the Haversian bone are oriented in the directions of dominant 1st principal stresses and ca in the directions of dominant 1st principal deformations also. In the left wall of the right femoral diaphysis, longitudinal osteon axes are tangents to the left-handed helix and, in the right wall, to the right-handed helix[46,52,56].

("second") layer of "long" subnanofibrils lying in the plane parallel to the central plane of the previous (i.e. "first" layer) can be described in a similar way (Figure 3). Potential buckling of chained and parallel "long" subnanofibrils in individual layers is prevented by lateral HA nanoplates ca 3 nm in thickness, which have roughly rectangular areas with dimensions of ca (15 to 30) nm x 50 nm[41,50]. The HA nanoplates are composed of HA crystals having the same orientation of the first principal (non-polar) axes of crystal symmetry in the same nanoplate. The central plane of these flat HA nanoplates is parallel to the central planes of laminated chained subnanofibrils (Figure 3). The HA nanoplates have central planes oriented parallel to each other in each mineralized subnanofibril (Figure 3).

In terms of biomechanics, the systems (complexes) of "chained" mineralized subnanofibrils 1.23 nm in thickness, lying in parallel layers (of ca the same thickness) form (together with HA nanoplates) a composite mineralized nanofibril (*nanorod*), Figure 1. The mineralized nanofibril (*nanorod*) is the fundamental bearing element of the 2nd structural level of the cortical bone (Table 1). The cross sections of mineralized nanorods are circular/oval in shape (Figure 3, bottom right). The diameters of the circular cross sections roughly range from 80 to 140 nm in size, (Figure 1, and Figure 3). The mineralized fibril transfers tensile loads via tropocollagen molecules and compressive loads via polycrystalline HA blocks or polycrystalline HA nanoplates.

The mineralized nanoshell (Figure 5) is the fundamental structural unit of the 3rd structural level. Each mineralized nanoshell is composed of parallel oriented mineralized nanofibrils (*nanorods*) having roughly the same orientation in the same shell layer (Figure 2). In terms of biomechanics, mineralized nanoshells can transfer both dominant principal stresses in tension and dominant principal stresses in compression in the direction of the longitudinal axes of mineralized nanofibrils.

The *mineralized microfibre* (Figure 4, Figure 6, and Figure 7) is the fundamental structural domain of the 4th structural level. It is often formed by concentric and overlapping mineralized cylindrical annuluses or their segments. The thicknesses of individual *nanoshells* range around 80-140 nm. Whereas the orientations of nanorods in a single (nano)shell are roughly the same, in adjoining (lower) shells (in the direction towards the

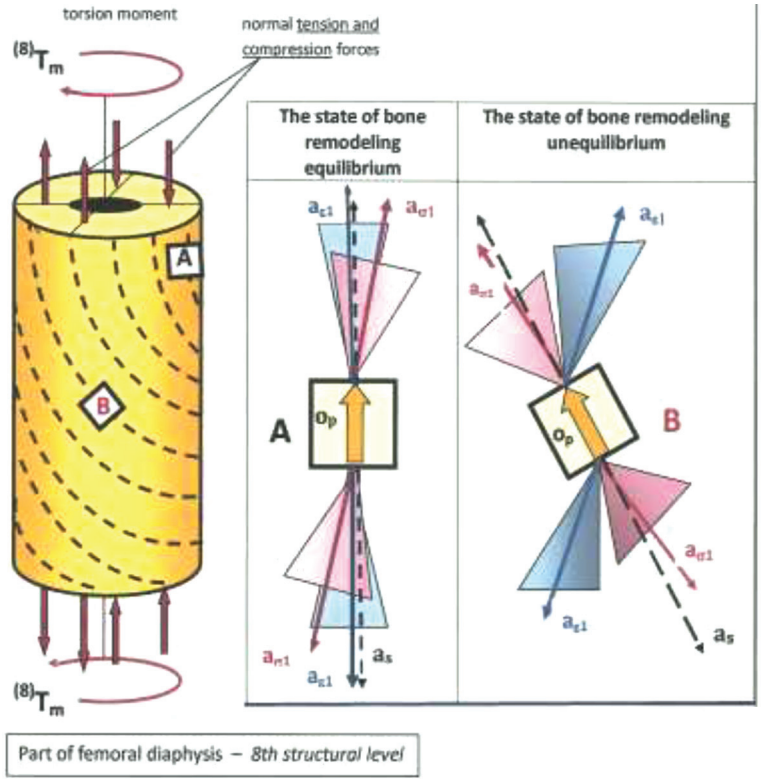


**Figure 11.** A schematic diagram illustrating a stable state in the cortical bone (at point **A**) and an unstable state in the bone (at point **B**) at beginning of the bone remodeling. The directions of dominant 1st principal stresses in the ideal state of the bone during a remodeling equilibrium are approximately identical with the first principal axis of anisotrophy, with the longitudinal axis of osteon and with the directions of dominant 1st principal strains. Unstable states (at point **B**) are initiated when all dominant principal axes are differently oriented[46,52-54]. *(Note: Triangular areas in Figure 11 denote the deflection field of dominant 1st principal stresses and dominant 1st principal deformations which may arise during the changes of combined bone tissue loadings).*

centre of the mineralized microfibre) there are noticeable deviations in their orientation. According to our findings, individual sublayers of mineralized helical nanoshells form a sandwich-like composite column structure with oriented nanofibrils Figure 2, Figure 5.

In 1988, Giruad-Guille described structures of lamellae composed of sublayers (within the whole lamella) and denoted them TPA (Twisted Plywood Architecture)[22,23]. The orientations of nanofibrils in sublayers differ. In other words, in successive sublayers, their inclination increases/decreases according the intensity of their loading. Girard-Guille's observations and conclusions correspond to our observations of lamellae positioned closer to the osteon's centre where the oval cross sections of cylindrical microfibres are rather planar or only slightly rounded.

In terms of biomechanics, due to the shear (tangential) stresses exerted by external torsion moments, the components of mineralized nanoshells (i.e. mineralized microfibres) are loaded by microtensions transferred by collagen fibres and by multidirectional microcompressions transferred by polycrystalline HA complexes.

The *osteon lamella* is the fundamental constitutive structural domain of the 5th structural level (Figure 8). The thickness of concentric lamellae mostly ranges in the interval of ca 5-8 μm (sometimes up to 15 μm). There are some differences appearing in the descriptions of the structures of osteon lamellae in publications. The terms "fibre" and "bone lamella" (at the 4th and 5th structural level) have been described in professional literature from several, more or less different perspectives (mostly as a consequence of using a specific device and method) as follows:

1) The lamellar osteon unit (under the polarized light microscope, PLM) is composed of alternating light and dark layers[11,51].
2) The lamellar osteon unit (under the optical microscope, OM) is composed of alternating thick and thin layers[15].
3) The lamellar unit is composed of several sublayers (sublamellae)[39,40,43].

4) The lamellar unit is composed of sublayers in which the orientation of fibrils changes in each successive sublayer (Twisted Plywood Architecture)[22-25].

According our studies, the lamellae are composed of mineralized microfibres (*microcolumns*), Figure 6, Figure 7, interconnected by mineralized shell fans and/or microshell plates (Figure 5, Figure 6). Column walls (*lamellae*) form a complex bearing element – an osteon. Normal tensile/compressive forces, bending and torsion moments are transferred to the lower structural levels of microfibres.

The fundamental structural domain of the cortical bone at the 6th structural level is the osteon (Figure 9). Its structure has been described by numerous authors since the second half of the 19th century[3] up to[10,15,20,22,39,43,46] and many others. The osteon is a microstructural bone tissue element, very roughly cylindrical in shape, with the outside diameter of ca 200 to 300 μm. Different views of the structures were mostly caused by the fact that the observation apparatus used and the observation methods selected had been designed for specific applications. Therefore, starting from the end of the second half of the 19th century, more or less different descriptions of osteon submicrostructures have appeared[47]. As a consequence of the validity of the dynamic remodeling equilibrium principle, the longitudinal axes of osteons are oriented in the directions of dominant first principal stresses (or dominant first principal deformations), Figure 10, Figure 11[46,52,53].

The systems of osteons and interstitial lamellae form the 7th structural level – mesostructure of bone tissue. This structural level includes systems with randomly localized osteons which mutually touch upon each other or are separated by interstitial lamellae, which are the remains of previous generations of osteonal structures, Figure 9. The interstitial lamellae have a higher content of mineral components and a relatively higher modulus of elasticity in compression than the adjoining osteon lamellae. The mesostructure is dominantly loaded by variations of combinations of normal and shear forces, bending and torsion moments. All combined loading effects are transferred and gradually dissipated into lower structural levels depending on the loading intensity. The osteons near the periost are loaded not only by tensions/compressions, but also by torsion moments. It is evident that *external torsion moments affect not only the orientations of osteons, but also the orientations of their lamellae, the orientation of microfibres and the orientations of nanofibrils in shell segments at lower structural levels*.

At the 7th structural level, like at each lower level of the cortical bone, in terms of biomechanics, its structures are the reflection of its adaptation to external biomechanical effects. The dominant directions of principal stresses/principal deformations correspond to the dominant biomechanical effects at the respective structural level (and the monitored locality). The principal bearing components, such as, e.g. osteons at the 7th structural level, are oriented in these directions in remodeling cycles[46]. In other words, the longitudinal axes of osteons are oriented identically in the direction of the *first dominant principal stress/principal strain and in the direction of the dominant first principal axis of anisotropy*.

The bone tissue remodeling (in the given locality) tends to the state of *remodelling equilibrium* (Figure 11, at point A), i.e. at the state of identity (or approximation) of the directions of: (1) the dominant first principal stress $\boldsymbol{\sigma}_1$ / the dominant first principal strain $\boldsymbol{\varepsilon}_1$, (2) the first principal axis of anisotropy $\boldsymbol{a}_1$ and (3) the longitudinal axis of the osteon structure - $\boldsymbol{o}_1$. Due to the fact the femoral diaphysis (e.g. while walking or running) is also loaded by the torsion moment (apart from bending moments, normal and shear forces), the osteons of the right femoral diaphyses have the orientation of a *left-handed helix in the medial wall of* the diaphysis and *a right-handed helix in the lateral wall*[46]. Anisotropic properties of cortical bone and helical (left-handed and right-handed) orientations of osteons in femoral walls at the 7th structural level are the proof of the *nonlinear anisotropy of the diaphyseal human bone*[46,52,53,57].

In this context, it should be mentioned that for example effects of external torsion moments are transferred from the 7th structural level to the 4th and also 3rd structural level. Due to the effects of torsion macro/micromoments, the structures with the helical orientation of bearing domains arise. Therefore, the domains at the 4th structural level (i.e. the mineralize microfibres) have *locally nonlinear anisotropy*.

## Conclusions

On the basis of our observations and the analyses of nanostructures and submicrostructures of femoral bone osteons, the following most important conclusions can be drawn:

1) The fundamental structural domain of the 3rd structural level is the mineralized nanoshell (Figure 5) 80-140 nm in thickness. The nanoshell is composed of parallel mineralized fibrils (nanorods), (Figure 1 and Figure 2). Nanoshells form laminated (mutually wrapping each other) cylindrical annular segments. In each (individual) nanoshell, the nanofibrils have roughly the same orientation. In adjacent layers, however, the orientations of nanofibrils tend to differ.
2) The mineralized microfibre (*microcolumn*) is the fundamental bearing domain of the 4th structural level. It is composed of the nanolayers of segments of cylindrical nanoshells (Figure 5, Figure 6 and Figure 7).
3) Adjacent microcolumns (within the same osteon lamella) are interconnected via mineralized laminated fan-shaped shells and/or mineralized laminated nanoplates in the tangential direction where individual layers reach nanothicknesses (Figure 5 and Figure 6).
4) The domain of the 5th structural layer is the osteon lamella (*a mineralized column wall*), which is formed by roughly parallel, equally oriented mineralized microfibres

– microcolumns. Microcolumns are mostly found in the lamellae more distant from the Haversian canal. In the lamellae closer to the Haversian canal, the columns get flatter and create wall structures composed of laminated shell plates.

5) Adjacent lamellae are mutually cross-linked (in the interlamellar space) by cantilever multi-laminated shells in the radial direction. The interlamellar space (between two adjacent lamellae) contains discrete shell bindings which stabilize adjacent lamellae in the radial direction.
6) Radial and tangential shells increase not only the stability of mineralized microfibres, but also the bending and torsion spatial rigidity of each osteon. The systems of lamellar column walls may transfer combined loads, i.e. combinations of the effects of torsion moments, bending moments and compressive/tensile normal forces. Torsion moments contribute to the formation of helical structures in the femoral cortical bone.
7) The presented results may become very useful in near future for modern bone tissue replacements based on nanofibrils and nanoparticles[37,38], applied mainly at older patients.

*Acknowledgements*

*This study was supported by the Ministry of Education: Transdisciplinary Research in Biomedical Engineering II, No.: MSM 684077O012 and by the Department of Composite and Carbon Materials, The Institute of Rock Structures and Mechanics, Academy of Sciences in Prague.*

## References

1. Takano Y, Turner CH, Owan I, Martin RB, Lau ST, Forwood MR, Burr DB. Elastic anisotropy and collagen orientation of osteonal bone are dependent on the mechanical strain distribution. J Ortop Research 1999;17(1):59-6.
2. Robling AG, Castillo AB, Turner CH. Biomechanical and molecular regulative of bone remodelling. Annual Rev Biomed Eng 2006; 8:455-98.
3. Gebhardt W. Über funktionell wichtige Anordnungsweisen der gröberen und feineren Bauelemente des Wirbeltierknochens. In: Archiv für Entwicklungsmechanik der Organismen. 1901;11:383-498 und In: Spezieller Teil 1. Der Bau der Haverssohen Lamellensysteme und seine funktionelle Bedeutung. Arch Entwickl Mech Org 1906;20:187-322.
4. Weindenreich J. Das Knochengewebe. In: Handbuch der mikroskopischen Anatomie des Menschen. Berlin: Springer; 1930, p. 391-520.
5. Ranvier L. Traité Technique d'Histologie. Paris: Savy F; 1887.
6. Ziegler D. Studien uber die feinere Struktur des Rohrenknochens und dessen Polarization. Dtsch Z Chir 1908;85:248-62.
7. Ruth EB. Bone studies. I. Fibrillar structure of adult human bone, Am J Anat 1947;80:35-53.
8. Rouillier CH, Huber L, Kellenberger ED, Rutishauser RE. La structure lamellaire de l'ostéon. Acta Anat 1952;14:9-22.
9. Rouillier CH. Collagen fibres of connective tissue. In: Biochemistry and Physiology of Bone. London: Academic Press; 1956. p.107-47.
10. Ascenzi A, Bonucci E. A quantitative investigation of the birefringence of the osteon. Acta Anat 1961;44:236-62.
11. Ascenzi A, Bonucci E. The tensile properties of single osteon. Anat Res 1967;57:378-86.
12. Ascenzi A, Bonucci E. The compressive properties of single osteon. Anat Res 1968;61:377-82.
13. Ascenzi A, Bonucci E. Simkin A. An approach to the mechanical properties of single osteon lamellae, J Biomech 1973;6: 227-35.
14. Ascenzi MG. A first estimation of prestress in so-called circularly fibered osteonic lamellae. J Biomech 1999;32:935-42.
15. Marotti G, Muglia MA. A scanning electron microscopic study lamellar organization. Arch Ital Anat Embriol 1988;93:163-75.
16. Marotti G, Muglia MA, Palumbo C, Zaffe D. The microscopic determinants of bone mechanical properties. Ital J Miner Electr Metab 1994;8:167-75.
17. Marotti G, Ferretti M, Palumbo C. The problem of bone lamellation: an attempt to explain different proposed models. J Morphol 2013; 274(5):543-50.
18. Marotti G, Muglia MA, Palumbo C. Collagen texture and osteofyte distribution in lamellar bone. Ital J Anat Embryol 1995;100 Suppl 1:95-102.
19. Marotti G. A new theory of bone lamellation. Calcif Tissue. 1993; 53:Issue 1, Supplement S47-S56.
20. Reid SA. A study of lamellar organization in juvenile and adult human bone. Anat Embryol 1986;174:329-38.
21. Marotti G. The structure of bone tissues and the cellular control of their deposition. Ital J Anat Embryol 1996;101:25-79.
22. Giraud-Guille MM. Twisted plywood architecture of collagen fibrils in human compact bone osteon. Calcif Tissue Int 1988;42(3):167-80.
23. Giraud-Guille MM, Besseau L, Martin R. Liquid crystalline assemblies of collagen in bone and in vitro system. J Biomech 2003;36(10):1571-79.
24. Hofmann T, Heyroth F, Meinhard H, Frazel W, Raum K. Assessment of composition and anisotropic elastic properties of secondary osteon lamellae. J Biomech 2006;39(12):2282-94.
25. Wagermaier W, Gupta HS, Gourrier A, Burghammer M, Roschger P, Fratzl P. Spiral twisting of fibre orientation inside bone lamellae. Biointerphase 2006;1(1):1-5.
26. Landis WJ. The strength of the calcified tissue depends in part on the molecular-structure and organization of its constituent mineral crystals in their organic matrix. Bone 1995;15:533-544.
27. Weiner S, Traub W. Organization of hydroxyapatite crystals within collagen fibrils. Febs Letters 1986:206-262.
28. Groot K. Effect of porosity and physicochemical properties on the stability, resorption, and strength of calcium phosphate ceramics. Ann Acad Sci 1988;523:227-33.
29. Thula TT, Rodrigues DE, Lee DE, Pendi L, Podschun J, Gower LB. In vitro mineralization of dense collagen substrates: A biomimetic approach toward the development of bone graft materials. Acta Biomater 2011;7:3158-3169.
30. Traub W, Arad T, Weiner S. Three-dimensional ordered distribution of crystals in turkey tendon collagen fibres. Pro Nat Acad Sci USA 1989;86:9822-26.
31. Landis WJ, Hodgens KJ, Song MJ, Arena J, Kionaga S, Marko M, Owen C, McEwen F. Mineralization of collagen may occur on fibril surfaces: Evidence from conventional and high-voltage electron microscopy and three dimensional imaging. Journal of Structural Biology 1996;117: 24.
32. Antebi B, Cheng X, Harris JN, Gower LB, Cheng XD, Ling J. Biomimetic collagen-hydroxyapatite composite fabricated via a novel perfusion-flow mineralization technique. Tissue Eng 2013;19:487-96.
33. Jia M, Hong Y, Duan S, Liu Y, Yuan B, Jian F. The influence of transition metal ions on collagen mineralization. Mat Sci Eng C Mater Biol Appl

2013;33:2399-2406.
34. Eyre DR, Weis MA. Bone collagen: new clues to its mineralization mechanism from recessive osteogenesis imperfecta. Calcif Tissie Int 2013;93:338-47.
35. Rho JY, Kuhn-Spearing L, Zioups P. Mechanical properties and the hierarchical structure of bone. Med Eng Phys 1998;20(2):92-102.
36. Hamed E, Lee Y, Jasiuk I. Multiscale modelling of elastic properties of cortical bone. Acta Mech 2010;213:131-54.
37. Supova M. Substituted hydroxyapatites for biomedical applications. Ceramics International 1915;41(8):9203-31.
38. Suchy T, Supova M, Sauerova P, Verdanova M, Sucharda Z, Ryglova S, Zaloudkova M, Sedlacek R, Kalbachova MH. The effect of different cross-linking conditions on collagen-based nanocomposite scaffolds - an in vitro evaluation using mesenchymal stem cells. Biomedical Materials 2016;10:2-14/065088.
39. Weiner S, Traub W, Wagner HD. Lamellar bone: structure-function relations. J Struct Biol 1999;126:241-56.
40. Weine S, Arad T, Sabanay I, Traub W. Rotated plywood structure of primary lamellar bone in the rat: orientation of collagen fibril arrays. Bone 1997;20(6):509-14.
41. Landis WJ, Song MJ, Leith A, McEwen F. Mineral and organic matrix interaction in normally calcified tendon visualized in 3 dimensions by high-voltage microscopic tomography and graphic image-reconstruction. Journal of Structural Biology 1993;110:39.
42. Tomoaia G, Pasca RD. On the collagen mineralization, a review. C Medical 2015;88(1):15-22.
43. Ziv V, Sabanay I, Arad T, Traub W, Weiner S. Transitional structures in lamellar bone. Microscop Re and Tech 1996;33:203.
44. Olsyta MJ, et al. Bone structure and formation: a new perspective. Mater Sci Eng Rep 2007;58:77-116.
45. Granke M, Gourier A, Rupin F, Raum K, Burghammer M, Saled A, Laugier P. Microfibril orientation dominates microelastic properties of human bone tissue at the lamellar length scale. Plos One 2013; 3(8):1-11.
46. Petrtyl M, Hert J, Fiala P. Spatial organization of the Haversian bone in man. Journal of Biomechanics 1996;29(2):161-69.
47. Robling AG, et al. Biomechanical and molecular regulative of bone remodelling. Ann Rev Biomed Eng 2006;8:455-98.
48. Trau W, Ara T, Weiner S. Growth of mineral crystals in turkey tendon collagen-fibres. Connective Tissue Re 1992;28:99.
49. Hengsberger S, Kulik A, Zysset PK. Nanoindentation discriminates the elastic properties of individual human bone lamellae under dry and physiological conditions. Bone 2002;30(1):178-84.
50. Landys WJ, Hodgens KJ, Arena J, Song MJ, McEwen BF. Structural relation between collagen and mineral in bone as determined by high voltage electron microscopic tomography. Microsc Res Tech 1996;33(2):192-202.
51. Ascenzi MG, Ascenzi A, Benvenuti A, Burghammer M, Pauzavolta S, et al. Structural differences between "dark" and "bright" isolates human osteonic lamellae. J Struct Biol 2003;141(1): 22-3.
52. Hert J, Fiala P, Petrtyl M. Osteon orientation of the diaphysis of the long bones in man. Bone 1994;15(3):269-77.
53. Petrtyl M. Curvilinear anisotropic properties of compact femoral bone. Proc 2nd Conf on Biomech of Man Liblice 1988, 123-26 (in Czech).
54. Hert J, Fiala P, Petrtyl M. Structure of compact bone and stress of which long bones in man are exposed. Acta Chirurg Orthop et Traumat CechosI 1990;80:199-208 (in Czech).
55. Wang M. Bioactive materials and processing. In: Shi D (Ed.) Biomaterials and tissue engineering. Berlin-Heidelberg-New York: Springer, 2004. p. 1-246.
56. Petrtyl M. Reactivities of the Compact Femoral Bone to the External Load. In: Proceedings of the 24th Congress of Biomech. Paris. 1993; 1028-29.
57. Petrtyl M. Spiral Flow of Elastic Properties in the Compact Femoral Bone, In: Proceedings of the 25th Congr of Eur Soc Artif Organs. Prague. 1988;141-45.